 doi:10.20944/preprints202207.0220.v1

HepG2-NTCP subclones exhibiting high susceptibility to hepatitis B virus infection

Muhammad Atif Zahoor[1], Adrian Kuipery[1, 2], Alexander I. Mosa[1], Adam J. Gehring[1, 2] and Jordan J. Feld[1]*

[1]Toronto Center for Liver Disease, Toronto General Hospital Research Institute, University Health Network, University of Toronto, Canada

[2]Department of Immunology, University of Toronto, Toronto, Ontario, Canada

Running title: Improved HepG2-NTCP HBV *In Vitro* Infection Model

Key words: Hepatitis B virus, HepG2-NTCP cells, Immunofluorescence, Sodium taurocholate cotransporting polypeptide (NTCP) Receptor, Subcloning, Limiting dilution, Myrcludex B

Word count

Abstract: **213**

Text: (Including the list of references, figure legends and the table): **4160**

*Correspondence: Jordan J. Feld, Toronto Center for Liver Disease (TCLD), Toronto General Hospital Research, 13 Institute (TGHRI), MaRS-Princess Margaret Cancer Research Tower 10-401, University Health 14 Network (UHN), 101-College St. Toronto, ON M5G 1L7. Email to: jordan.feld@uhn.ca

 doi:10.20944/preprints202207.0220.v1

ABSTRACT

HepG2 cells reconstituted with Hepatitis B virus (HBV) entry receptor sodium taurocholate co-transporting polypeptide (NTCP) are widely used as a convenient *in vitro* cell culture infection model for HBV replication studies. As such, it is pertinent that HBV infectivity is maintained at steady-state levels for accurate interpretation of *in vitro* data. However, variations in HBV infection efficiency due to imbalanced NTCP expression levels in the HepG2 cell line may affect experimental results. In this study, we performed single cell cloning of HepG2-NTCP-A3 parental cells via limiting dilution and obtained multiple subclones with increased permissiveness to HBV. Specifically, one subclone (HepG2-NTCP-A3/C2) yielded more than 4-fold higher HBV infection compared to the HepG2-NTCP-A3 parental clone. In addition, though HBV infectivity was universally reduced in the absence of polyethylene glycol (PEG), subclone C2 maintained relatively greater permissiveness under PEG-free conditions, suggesting the functional heterogeneity within parental HepG2-NTCP-A3 may be exploitable in developing a PEG-free HBV infection model. The increased viral production correlated with increased intracellular viral antigen expression as evidenced through HBcAg immunofluorescence staining. Further, these subclones were found to express different levels of NTCP, albeit with no remarkable morphology or cell growth differences. In conclusion, we isolated subclones of HepG2-NTCP-A3 which support efficient HBV production and thus provide an improved *in vitro* HBV infection model.

Preprints (www.preprints.org) | NOT PEER-REVIEWED | Posted: 14 July 2022 doi:10.20944/preprints202207.0220.v1

INTRODUCTION

Hepatitis B virus (HBV) infection is a major health problem worldwide, with 3.5% of the global population chronically infected. Though infections in adulthood are typically acute and self-resolving, chronic infection is characterized by persistent, asymptomatic liver inflammation leading to progressive fibrosis that may culminate in severe complications, such as cirrhosis and hepatocellular carcinoma [1,2]. Although, HBV is vaccine-preventable and current therapy with nucleos(t)ide analogues (NUCs) can suppress virus replication, treatment is usually life-long and viral clearance is rare. Nearly one million people die every year due to HBV-related complications [3]

With narrow host and tissue specificity, *in vitro* models permissive to HBV are critical tools in understanding viral replication and designing curative therapies. Though hepatoma lines have been used for decades to study HBV replication, recent advances using HepG2 cells reconstituted with the HBV receptor sodium taurocholate co-transporting polypeptide (NTCP) have provided an accessible, standardized *in vitro* model for HBV infection [3–6]. We hypothesized that subpopulations within this model would manifest variability in permissiveness to HBV. This is an important consideration in reducing inter and intra-experimental variability, as varying representation of subpopulations within a culture may skew efficacy of candidate antivirals and susceptibility to infection. Further, selective culturing of subpopulations with increased permissiveness could increase the reproducibility and efficiency of the HepG2-NTCP *in vitro* model. In this study, we performed subcloning of the HepG2-NTCP-A3 parental clone and obtained subclones which exhibited variations in permissiveness to HBV infection. We isolated the most permissive line and observed increased expression of NTCP relative to the parental line.

Preprints (www.preprints.org) | NOT PEER-REVIEWED | Posted: 14 July 2022 doi:10.20944/preprints202207.0220.v1

Collectively, these findings suggest this subclone provides an improved HBV infection model, and that parental HepG2-NTCP subpopulations should be routinely screened to reduce intra-lineage variability in HBV permissiveness.

MATERIALS AND METHODS

Generation of HepG2-NTCP subclones

HepG2 and HepG-NTCP-A3 cells were cultured in Dulbeco's Modified Eagles Medium (DMEM; Sigma-Aldrich) supplemented with 10% fetal bovine serum (FBS) (GIBCO, Canada), L-glutamine, 100U penicillin/ streptomycin (Gibco Fisher Scientific, Canada), 1mM Sodium Pyruvate, 20mM HEPES, essential and non-essential amino acids (Corning, Manasas, VA, USA) and 5 µg plasmosin (Invivogen, Cedarlane, Canada) at 37^{o}C in a 5% humidified incubator as described [7]. HepG2-NTCP-A3 subclones were obtained by limiting dilution essentially as described [8]. Briefly, a total of 96 cells in 20 ml media containing 2.5 µg/ml puromycin were seeded at 200 ul per well into a 96 well plate. After two weeks, single cell clones were isolated, expanded and stored at -196^{o}C until further use.

NTCP Expression

HepG2-NTCP-A3 subclones were expanded and total RNA was isolated using the RNeasy mini kit (QIAgen, Canada). RNA concentration was measured by nanodrop and subjected to cDNA synthesis as described [9]. The amounts of NTCP and GAPDH mRNAs were estimated by quantitative real-time PCR as described [10] with Quant

Preprints (www.preprints.org) | NOT PEER-REVIEWED | Posted: 14 July 2022 doi:10.20944/preprints202207.0220.v1

Studio 6 Flex system (Thermo Scientific, Canada) using the primer pairs 5′-CTCTCTTCTGCCTCAATGGAC-3′ and 5′-CAGTTGTGGCAGCTGTGTAG-3′ and 5′-GAAGGTCGGAGTCAACGGATT-3′ and 5′-TGATGACAAGCTTCCCGTTCTC-3′, respectively.

Peptide labelling and staining of NTCP expressing cells

Myrcludex B (MyrB), a lipopeptide consisting of amino acid residues 2-48 of the pre-S1 region of the HBV large surface antigen [11] was labelled with Alexa Flour 647 protein labeling kit according to the manufacturer's instructions (Thermo Scientific, Canada) and designated as MyrB-Alexa-647. For staining of NTCP expression, HepG2, HepG2-NTCP-A3 parental clone or its subclones B7, C2, D10, G4 and G7 were seeded into a 12-well plate and incubated with 200nM MyrB-Alexa-647 at 37ºC for 30 minutes as described [12,13]. Unbound peptide was removed by washing with 1xPBS, the cells were fixed with 4% paraformaldehyde (PFA) and imaged using EVOS FL-Auto 2 fluorescence microscope (Invitrogen, Canada) as described [7].

HBV infection and HBV DNA quantification

HepG2-NTCP-A3 parental clone or its subclones were seeded at 500,000 cells per ml per well into a 12-well plate and infected with HepAD38-cell harvested HBV genotype D at 100, 200, 500 or 1000 Genome Equivalents (GEq)/ml in the presence of 2.5% dimethyl sulfoxide (DMSO; Sigma) and 4% or no polyethylene glycol (PEG 8000; Sigma) as described [7,14–16]. The next day, the virus inoculum was removed, the cells were extensively washed with PBS and cultured in the presence of DMSO-2.5%. Four days post-infection, viral DNA was extracted from supernatants using the DNeasy blood & tissue kit (QIAgen, Canada) according to the manufacturer's instructions and quantified

Preprints (www.preprints.org) | NOT PEER-REVIEWED | Posted: 14 July 2022 doi:10.20944/preprints202207.0220.v1

using HBV 1844F 5'-GTTGCCCGTTTGTCCTCTAATTC-3' as a forward and HBV 1745R 5'-GGAGGGATACATAGAGGTTCCTTGA-3' as a reverse primer as described [17] with Quant Studio 6 Flex system (Thermo Scientific, Canada). HBV 1.3-mer plasmid DNA (Addgene # 6820) was used as a standard to calculate the amount of HBV DNA. With written informed consent and our institutional study ethics approval (Ethical review committee: UHN Ethics Board; Approval number: 53418), serum samples from three chronically infected HBV patients with a viral load of $3.42\pm2.11x10^8$ GEq/ml were obtained from the Toronto Center for Liver Disease as described [18]. DNA was extracted as described above and the viral surface gene was amplified with 5′-TCACCATATTCTTGGGAACAAGA-3′ and 5′-CGAACCACTGAACAAATGGC-3′ as forward and reverse primers, respectively. The PCR product was sequenced using 5′-TGGGAACAAGAGCTACAGCATGG-3′ as a sequencing primer and the genotypes were determined using the NCBI genotyping online tool as described [19]. Crude and unpurified serum samples are known to reduce HBV infectivity [16], therefore; serum samples were buffer exchanged using Amicon Ultra 0.5µM filter units (Sigma, Oakville, Canada) by centrifugation at 13,000 rpm for 30 min as described [20] and used to infect HepG2-NTCP-A3 parental and C2 subclone at 500 GEq/ml for 24 hrs. The next day, the virus inoculum was removed, and the infected cells were maintained for 7 days in the presence of 2.5% DMSO. The viral DNA was extracted from the cell culture supernatant and quantified as described above.

Immunofluorescence for HBV core protein

HepG2-NTCP-A3 parental clone or its subclones were cultured and infected with HBV as described above. Cells were fixed in 4% PFA at room temperature, washed with PBS and

Preprints (www.preprints.org) | NOT PEER-REVIEWED | Posted: 14 July 2022 doi:10.20944/preprints202207.0220.v1

permeabilized with 0.5 % Triton X-100. After blocking, cells were incubated with rabbit polyclonal HBV anti-Core antibody C149 at 1:5000 dilution as described [21] as a primary and donkey anti-rabbit Alexa fluor-647 at 1:500 dilution (Thermo Scientific, Canada) as a secondary antibody. Nuclei were stained with DAPI and the cells were imaged using EVOS FL Auto 2 (Invitrogen, Canada) as described [7].

Statistical Analysis

The analyses were carried out using GraphPad Prism (San Diego, CA, USA) as described [9]. Data are shown as mean ± SD.

RESULTS

Enhanced HBV infection in subclones of HepG2-NTCP cells

To obtain subclones of HepG2-NTCP-A3 with enhanced HBV infectivity, we performed subcloning through limiting dilution and obtained twelve subclones. Two clones showed irregular morphology and did not grow. We expanded five subclones designated as B7, C2, D10, G4 and G7, infected each with HBV overnight, with or without PEG8000, and then cultured in growth media for an additional three days. Extracellular HBV DNA was assessed in the culture supernatant. Results showed that following HBV infection in the presence of PEG8000, subclones B7, C2, D10, G4 and G7 yielded 2.98, 4.45-, 2.8-, 2.57- and 2.25-fold significantly higher HBV infectivity than the parental HepG2-NTCP-A3 clone (Fig 1A; Table 1). These data suggested that subcloning improved HBV permissiveness. Next, we performed IFA of HBV-infected subclones and observed, in agreement with our

Preprints (www.preprints.org) | NOT PEER-REVIEWED | Posted: 14 July 2022 doi:10.20944/preprints202207.0220.v1

qPCR data, that HBV was more infectious in HepG2-NTCP-A3 subclones (Fig 1B, 1C & Table 1).

Next, we selected the most permissive subclone C2 to determine if the enhanced infectivity was observed across different multiplicities of infection (MOI). We found that C2 was more permissive than the parental clone across a range of MOI, with the greatest proportional and absolute increases at MOI of 200 and 500, respectively (Fig 1D-1F). Our data suggest that the C2 subclone showed significantly higher levels of viral DNA and enhanced infectivity, however high MOI is still required for efficient HBV infectivity.

To investigate PEG-free HBV infection efficiency, subclones B7, C2, D10, G4, G7 and the parental clone HepG2-NTCP-A3 were infected with HBV overnight in the absence of PEG. Extracellular HBV DNA was assessed in the culture supernatant. Results showed that, compared to 4% PEG8000 (Fig 1), HBV infection was significantly lower in PEG-free conditions (Fig 2A-2C; Table 1). However, subclone C2 maintained greater permissiveness to HBV infection in PEG-free conditions than either the parental clone or the other subclones (Table 1), with a relative increase in infection efficiency under PEG-free conditions, suggesting the C2 subclone can be utilized if PEG-free conditions are required.

To determine if the enhanced permissiveness of C2 was limited to a single HBV genotype, which would imply that the permissive phenotype was a property emergent from a genotype-subclone interaction, rather than an intrinsic feature of the subclone, we evaluated infectivity using three patient-derived HBV isolates. Across genotypes B, C, and E, we observed enhanced permissiveness in the C2 subclone, though the absolute

 doi:10.20944/preprints202207.0220.v1

increase in infectivity was variable across genotypes (Fig 3A-3C), suggesting both intrinsic and emergent properties contribute to C2's increased permissiveness.

NTCP expression in subclones of HepG2-NTCP cells

To evaluate if NTCP expression varied between the most permissive subclones and the parental lineage, subclones B7, C2, D10, G4 and G7 and HepG2-NTCP-A3 were expanded, and NTCP mRNA expression levels were analyzed by qRT-PCR. Results showed that B7, C2 and D10 subclones expressed greater levels of NTCP compared with the HepG2-NTCP-A3 parental clone (Fig 4A). To examine whether relative expression of NTCP by HepG2-NTCP-A3 parental clone or its subclones correlated with HBV preS1 binding, we analyzed binding of MyrB-Alexa-647 by fluorescence microscopy. C2 and G7 subclones had the highest and the lowest MyrB binding compared to HepG2-NTCP-A3 parental clone, respectively, and the differences were statistically significant (Fig 4B & 4C). In addition, no morphological or growth differences between the subclones and the parental clone were observed, indicating that alteration in NTCP expression levels are independent of morphology and growth differences. Further, NTCP expression and permissiveness to HBV infection were only moderately correlated, implying that additional cellular factors, independent of NTCP expression, may influence HBV permissiveness (Fig 4D).

Preprints (www.preprints.org) | NOT PEER-REVIEWED | Posted: 14 July 2022 doi:10.20944/preprints202207.0220.v1

DISCUSSION

The discovery of NTCP as a functional receptor for HBV has allowed the development of cell-culture based models suitable for the study of the HBV life cycle. Thus, HepG2-NTCP cells provide a convenient infection model for HBV infection that has been used extensively for drug development studies [4,5]. Given that NTCP is a bona fide receptor for HBV, any variation in its expression may affect the outcome and kinetics of HBV infection. Such an observation in our experimental setting prompted us to investigate the clonality of the HepG2-NTCP-A3 cell line. Using limiting dilution, we obtained multiple HepG2-NTCP-A3 subclones with varying degrees of permissiveness to HBV, suggesting that the parental HepG2-NTCP-A3 is indeed a mixed population of functionally distinct phenotypes (Fig 1A-1C).

Low levels of NTCP expression are known to render hepatocytes poorly permissive to HBV infection [22]. It has also been shown that enhanced HBV infection in HepG2-NTCP cells is NTCP-dependent [19]. We observed that NTCP expression differed between the subclones and the parental HepG2-NTCP-A3 (Fig 4A). We further showed that NTCP expression levels reflected by MyrB binding-determined-immunofluorescence were significantly higher only in the C2 subclone compared to the HepG2-NTCp-A3 parental clone (Fig 4B & 4C). However, the relationship between NTCP expression and permissiveness was not uniformly observed across other subclones, suggesting other cellular factors may be operative in regulation of HBV entry or replication [16,23–25]. This finding agrees with a previous report where NTCP-expressing subclones also showed similar binding affinity towards MyrB [16] suggesting that intracellular NTCP might be playing a role in promoting HBV infection. Alternatively, a non-receptor role of NTCP in

 doi:10.20944/preprints202207.0220.v1

promoting HBV infection has also been suggested [26]. The original parental HepG2-NTCP-A3 clone was generated in 2014 through lentiviral mediated transduction [12]; it is possible that successive passaging has altered its cellular characteristics and thus has affected its overall permissiveness to HBV. Understanding of non-receptor function(s) of NTCP is limited and requires further investigation.

The addition of PEG is not physiologically relevant to human infection as it creates a non-specific cell membrane fusion [20]. 4% PEG is usually added to the incubation medium and is known to enhance the HBV entry process by facilitating the viral attachment to cell surface heparan sulfate proteoglycans [20,27,28]. Although, the addition of PEG significantly enhanced HBV infection for all clones, which is in line with previous reports [17,19,20]; the C2 subclone performed better than all other reported clones and the HepG2-NTCP-A3 parental clone in supporting PEG-free HBV infection [19]. Indeed, the difference in permissiveness between C2 and the other clones was greater in PEG-free conditions than in the presence of PEG (Fig 2A-2C; Table 1). Thus, the C2 subclone could be utilized for PEG-free HBV infection studies and it is likely that additional subcloning might further optimize the reduced dependency on PEG, which would be a significant advance.

In addition to enhancing the infection of cell culture-derived HBV genotype D, the C2 subclone also showed enhanced infectivity with patient-derived HBV samples of genotype B and E relative to HepG2-NTCP-A3 parental clone. Interestingly, both HepG2-NTCP-A3 parental clone as well as C2 subclone showed reduced susceptibility to genotype C patient-derived serum. The cause for the low infectivity with genoptype C HBV is not clear, however similar observations of low infectivity of genotype C have been attributed to the

 doi:10.20944/preprints202207.0220.v1

presence of large proportion of non-infectious virus particles or low infectivity of genotype C [16,29].

Although the difference in cell growth could affect the outcome of HBV infection, we did not observe any difference in cell growth or in cellular morphology in any of the HepG2-NTCP-A3 subclones (Fig 4B). In a recent report, a slow growing HepG2-NTCP-Sec^{+} subclone which requires high viral inoculum of up to 5000 GEq/ml, is shown to possess amplified HBV infectivity [16]. However, considering the practical disadvantages of slow growth and requirement of high inoculum, the subclones described in the current study especially C2 are advantageous and provide a more efficient HBV infection model. Moreover, previously reported growth differences in HepG2-NTCP subclones, and observations of varying permissiveness reported in the current study, suggest functional heterogeneity exists within HepG2-NTCP cells [16]. Similar heterogeneity has been reported for Huh7 cells [30], another hepatoma cell line that is susceptible to HBV infection upon exogenous NTCP expression [28].

In conclusion, we demonstrate that enhancement of permissiveness through HepG2-NTCP subcloning provides an improved model for HBV infection studies. Since HepG2-NTCP cells are also used for assessment of novel HBV antivirals, our findings suggest hepatoma cell lines expressing NTCP should be routinely monitored for any variation in NTCP expression, or permissiveness to HBV, when studying the HBV life cycle.

ACKNOWLEDGEMENTS

We would like to thank Dr. Stephen Urban and Dr. Adam Zlotnick for kindly providing the Myrcludex B and HepG2-NTCP-A3 clone and HBV core Cp149 antibody, respectively.

REFERENCES

1. Razavi-Shearer, D.; Gamkrelidze, I.; Nguyen, M.H.; Chen, D.-S.; van Damme, P.; Abbas, Z.; Abdulla, M.; Abou Rached, A.; Adda, D.; Aho, I.; et al. Global Prevalence, Treatment, and Prevention of Hepatitis B Virus Infection in 2016: A Modelling Study. *The Lancet Gastroenterology & Hepatology* **2018**, *3*, 383–403, doi:10.1016/S2468-1253(18)30056-6.
2. Schweitzer, A.; Horn, J.; Mikolajczyk, R.T.; Krause, G.; Ott, J.J. Estimations of Worldwide Prevalence of Chronic Hepatitis B Virus Infection: A Systematic Review of Data Published between 1965 and 2013. *The Lancet* **2015**, *386*, 1546–1555, doi:10.1016/S0140-6736(15)61412-X.
3. Trépo, C.; Chan, H.L.Y.; Lok, A. Hepatitis B Virus Infection. *The Lancet* **2014**, *384*, 2053–2063, doi:10.1016/S0140-6736(14)60220-8.
4. El-Serag, H.B. Epidemiology of Viral Hepatitis and Hepatocellular Carcinoma. *Gastroenterology* **2012**, *142*, 1264-1273.e1, doi:10.1053/j.gastro.2011.12.061.
5. Yan, H.; Liu, Y.; Sui, J.; Li, W. NTCP Opens the Door for Hepatitis B Virus Infection. *Antiviral Research* **2015**, *121*, 24–30, doi:10.1016/j.antiviral.2015.06.002.
6. Sun, Y.; Qi, Y.; Peng, B.; Li, W. NTCP-Reconstituted In Vitro HBV Infection System. In; 2017; pp. 1–14.
7. Kuipery, A.; Sanchez Vasquez, J.D.; Mehrotra, A.; Feld, J.J.; Janssen, H.L.A.; Gehring, A.J. Immunomodulation and RNA Interference Alter Hepatitis B Virus-specific CD8 T Cell Recognition of Infected HepG2-NTCP. *Hepatology* **2021**, doi:10.1002/hep.32230.
8. Zahoor, M.A.; Philip, S.; Zhi, H.; Giam, C.-Z. NF- B Inhibition Facilitates the Establishment of Cell Lines That Chronically Produce Human T-Lymphotropic Virus Type 1 Viral Particles. *Journal of Virology* **2014**, *88*, 3496–3504, doi:10.1128/jvi.02961-13.
9. Zahoor, M.A.; Woods, M.W.; Dizzell, S.; Nazli, A.; Mueller, K.M.; Nguyen, P. v.; Verschoor, C.P.; Kaushic, C. Transcriptional Profiling of Primary Endometrial Epithelial Cells Following Acute HIV-1 Exposure Reveals Gene Signatures Related to Innate Immunity. *American Journal of Reproductive Immunology* **2018**, *79*, e12822, doi:10.1111/aji.12822.
10. Okuyama-Dobashi, K.; Kasai, H.; Tanaka, T.; Yamashita, A.; Yasumoto, J.; Chen, W.; Okamoto, T.; Maekawa, S.; Watashi, K.; Wakita, T.; et al. Hepatitis B Virus Efficiently Infects Non-Adherent Hepatoma Cells via Human Sodium Taurocholate Cotransporting Polypeptide. *Scientific Reports* **2015**, *5*, 17047, doi:10.1038/srep17047.

11. Gripon, P.; Cannie, I.; Urban, S. Efficient Inhibition of Hepatitis B Virus Infection by Acylated Peptides Derived from the Large Viral Surface Protein. *Journal of Virology* **2005**, *79*, 1613–1622, doi:10.1128/JVI.79.3.1613-1622.2005.
12. Ni, Y.; Lempp, F.A.; Mehrle, S.; Nkongolo, S.; Kaufman, C.; Fälth, M.; Stindt, J.; Königer, C.; Nassal, M.; Kubitz, R.; et al. Hepatitis B and D Viruses Exploit Sodium Taurocholate Co-Transporting Polypeptide for Species-Specific Entry into Hepatocytes. *Gastroenterology* **2014**, *146*, 1070-1083.e6, doi:10.1053/j.gastro.2013.12.024.
13. Chakraborty, A.; Ko, C.; Henning, C.; Lucko, A.; Harris, J.M.; Chen, F.; Zhuang, X.; Wettengel, J.M.; Roessler, S.; Protzer, U.; et al. Synchronised Infection Identifies Early Rate-limiting Steps in the Hepatitis B Virus Life Cycle. *Cellular Microbiology* **2020**, *22*, doi:10.1111/cmi.13250.
14. Le, C.; Sirajee, R.; Steenbergen, R.; Joyce, M.A.; Addison, W.R.; Tyrrell, D.L. In Vitro Infection with Hepatitis B Virus Using Differentiated Human Serum Culture of Huh7.5-NTCP Cells without Requiring Dimethyl Sulfoxide. *Viruses* **2021**, *13*, 97, doi:10.3390/v13010097.
15. Ladner, S.K.; Otto, M.J.; Barker, C.S.; Zaifert, K.; Wang, G.H.; Guo, J.T.; Seeger, C.; King, R.W. Inducible Expression of Human Hepatitis B Virus (HBV) in Stably Transfected Hepatoblastoma Cells: A Novel System for Screening Potential Inhibitors of HBV Replication. *Antimicrobial Agents and Chemotherapy* **1997**, *41*, 1715–1720, doi:10.1128/AAC.41.8.1715.
16. König, A.; Yang, J.; Jo, E.; Park, K.H.P.; Kim, H.; Than, T.T.; Song, X.; Qi, X.; Dai, X.; Park, S.; et al. Efficient Long-Term Amplification of Hepatitis B Virus Isolates after Infection of Slow Proliferating HepG2-NTCP Cells. *Journal of Hepatology* **2019**, *71*, 289–300, doi:10.1016/j.jhep.2019.04.010.
17. Ko, C.; Chakraborty, A.; Chou, W.-M.; Hasreiter, J.; Wettengel, J.M.; Stadler, D.; Bester, R.; Asen, T.; Zhang, K.; Wisskirchen, K.; et al. Hepatitis B Virus Genome Recycling and de Novo Secondary Infection Events Maintain Stable CccDNA Levels. *Journal of Hepatology* **2018**, *69*, 1231–1241, doi:10.1016/j.jhep.2018.08.012.
18. Chua, C.G.; Mehrotra, A.; Mazzulli, T.; Wong, D.K.; Feld, J.J.; Janssen, H.L.A.; Gehring, A.J. Optimized Ex Vivo Stimulation Identifies Multi-Functional HBV-Specific T Cells in a Majority of Chronic Hepatitis B Patients. *Scientific Reports* **2020**, *10*, 11344, doi:10.1038/s41598-020-68226-5.
19. Michailidis, E.; Pabon, J.; Xiang, K.; Park, P.; Ramanan, V.; Hoffmann, H.-H.; Schneider, W.M.; Bhatia, S.N.; de Jong, Y.P.; Shlomai, A.; et al. A Robust Cell Culture System Supporting the Complete Life Cycle of Hepatitis B Virus. *Scientific Reports* **2017**, *7*, 16616, doi:10.1038/s41598-017-16882-5.
20. Choijilsuren, G.; Jhou, R.-S.; Chou, S.-F.; Chang, C.-J.; Yang, H.-I.; Chen, Y.-Y.; Chuang, W.-L.; Yu, M.-L.; Shih, C. Heparin at Physiological Concentration Can Enhance PEG-Free in Vitro Infection with Human Hepatitis B Virus. *Scientific Reports* **2017**, *7*, 14461, doi:10.1038/s41598-017-14573-9.
21. Nair, S.; Zlotnick, A. HBV Core Protein Is in Flux between Cytoplasmic, Nuclear, and Nucleolar Compartments. *mBio* **2021**, *12*, doi:10.1128/mBio.03514-20.
22. Yan, Y.; Allweiss, L.; Yang, D.; Kang, J.; Wang, J.; Qian, X.; Zhang, T.; Liu, H.; Wang, L.; Liu, S.; et al. Down-Regulation of Cell Membrane Localized NTCP Expression in Proliferating Hepatocytes Prevents Hepatitis B Virus Infection. *Emerging Microbes & Infections* **2019**, *8*, 879–894, doi:10.1080/22221751.2019.1625728.

23. Iwamoto, M.; Saso, W.; Sugiyama, R.; Ishii, K.; Ohki, M.; Nagamori, S.; Suzuki, R.; Aizaki, H.; Ryo, A.; Yun, J.-H.; et al. Epidermal Growth Factor Receptor Is a Host-Entry Cofactor Triggering Hepatitis B Virus Internalization. *Proceedings of the National Academy of Sciences* **2019**, *116*, 8487–8492, doi:10.1073/pnas.1811064116.
24. Bouezzedine, F.; Fardel, O.; Gripon, P. Interleukin 6 Inhibits HBV Entry through NTCP down Regulation. *Virology* **2015**, *481*, 34–42, doi:10.1016/j.virol.2015.02.026.
25. Eller, C.; Heydmann, L.; Colpitts, C.C.; el Saghire, H.; Piccioni, F.; Jühling, F.; Majzoub, K.; Pons, C.; Bach, C.; Lucifora, J.; et al. A Genome-Wide Gain-of-Function Screen Identifies CDKN2C as a HBV Host Factor. *Nature Communications* **2020**, *11*, 2707, doi:10.1038/s41467-020-16517-w.
26. Li, J.; Zong, L.; Sureau, C.; Barker, L.; Wands, J.R.; Tong, S. Unusual Features of Sodium Taurocholate Cotransporting Polypeptide as a Hepatitis B Virus Receptor. *Journal of Virology* **2016**, *90*, 8302–8313, doi:10.1128/JVI.01153-16.
27. Gripon, P.; Diot, C.; Guguen-Guillouzo, C. Reproducible High Level Infection of Cultured Adult Human Hepatocytes by Hepatitis B Virus: Effect of Polyethylene Glycol on Adsorption and Penetration. *Virology* **1993**, *192*, 534–540, doi:10.1006/viro.1993.1069.
28. Yan, H.; Zhong, G.; Xu, G.; He, W.; Jing, Z.; Gao, Z.; Huang, Y.; Qi, Y.; Peng, B.; Wang, H.; et al. Sodium Taurocholate Cotransporting Polypeptide Is a Functional Receptor for Human Hepatitis B and D Virus. *Elife* **2012**, *1*, doi:10.7554/eLife.00049.
29. Ou, G.; He, L.; Wang, L.; Song, J.; Lai, X.; Tian, X.; Wang, L.; Zhang, K.; Zhang, X.; Deng, J.; et al. The Genotype (A to H) Dependent N-Terminal Sequence of HBV Large Surface Protein Affects Viral Replication, Secretion and Infectivity. *Frontiers in Microbiology* **2021**, *12*, doi:10.3389/fmicb.2021.687785.
30. Sainz, B.; Barretto, N.; Uprichard, S.L. Hepatitis C Virus Infection in Phenotypically Distinct Huh7 Cell Lines. *PLoS ONE* **2009**, *4*, e6561, doi:10.1371/journal.pone.0006561.

Preprints (www.preprints.org) | NOT PEER-REVIEWED | Posted: 14 July 2022 doi:10.20944/preprints202207.0220.v1

Table 1: Comparison of HBV infection in the presence or absence of PEG in HepG2-NTCP parental clone and its subclones

	4% PEG				No Peg			
	Extracellular HBV DNA		Intracellular HBV DNA		Extracellular HBV DNA		Intracellular HBV DNA	
	HBV DNA log_{10}Copies/mL (SD)	Fold Change vs Parental	HBcAg MFI	Fold Change vs Parental	HBV DNA log_{10}Copies/mL (SD)	Fold Change vs Parental	HBV DNA log_{10}Copies/mL (SD)	Fold Change vs Parental
HepG2-NTCP-A3	6.20 ± 5.52	1.0	69.1 ± 1.3	1.0	4.21 ± 2.15	1.0	16.1 ± 0.4	1.0
B7	**6.66 ± 4.94[a]**	2.98	84.7 ± 2.6	1.22	**4.43 ± 3.45[b]**	1.67	16.7 ± 0.4	1.03
C2	**6.84 ± 5.93[a]**	4.45	**93.0 ± 2.3[a]**	1.35	**4.77 ± 2.51[b]**	3.63	**24.7 ±1.5[b]**	1.48
D10	**6.65 ± 4.06[a]**	2.80	79.6 ± 1.3	1.15	**4.42 ± 2.43[b]**	1.63	20.4 ± 0.6	1.22
G4	**6.59 ± 4.07[a]**	2.57	77.3 ± 1.5	1.12	4.08 ± 2.17	0.74	16.6 ± 0.9	0.99
G7	**6.54 ± 5.37[a]**	2.25	74.6 ± 1.5	1.08	4.03 ± 2.79	0.67	10.1 ± 4.1	0.60

[a]Significantly different from 4% PEG control (HepG2-NTCP-A3) ($p<0.05$)
[b]Significantly different from No PEG control (HepG2-NTCP-A3) ($p<0.05$)

Preprints (www.preprints.org) | NOT PEER-REVIEWED | Posted: 14 July 2022 doi:10.20944/preprints202207.0220.v1

FIGURE LEGENDS

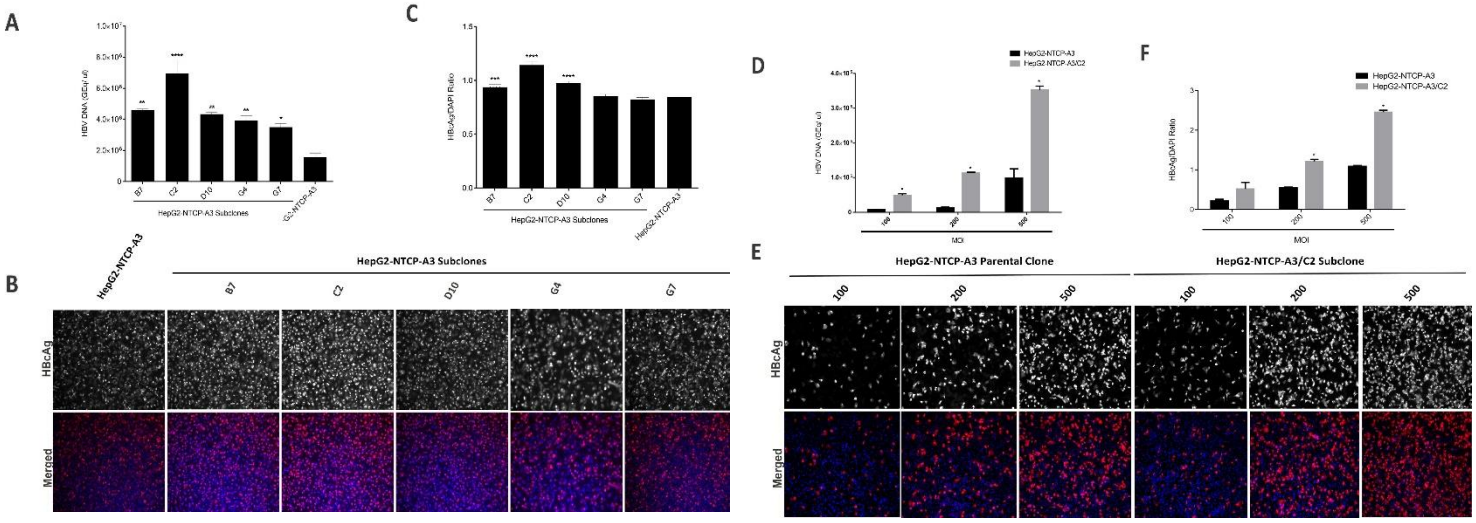

Figure 1: HBV infection in HepG2-NTCP-A3 subclones. A). Indicated subclones of HepG2-NTCP-A3 were infected with HBV at 1000 GEq/ml in the presence of PEG8000. Cell culture supernatants were collected, and the amount of HBV was quantified by real-time PCR B). HepG2-NTCP-A3 subclones infected with HBV were fixed and immunostained with an antibody to HBcAg and counterstained with DAPI. The cells were visualized by fluorescence microscopy C). HBcAg fluorescence over DAPI shown as a ratio. Data are presented as mean±SD (One way ANOVA; p <0.0001) D). C2 subclone and HepG2-NTCP-A3 parental clone were infected with HBV at 100, 200 and 500 MOI. Supernatants were collected at day 4 post-infection for DNA quantification E). The cells were fixed and immunostained with HBcAg antibodies and nuclei were counterstained with DAPI F). HBcAg fluorescence over DAPI shown as a ratio. Data are presented as mean±SD (t-test; p <0.005).

Preprints (www.preprints.org) | NOT PEER-REVIEWED | Posted: 14 July 2022 doi:10.20944/preprints202207.0220.v1

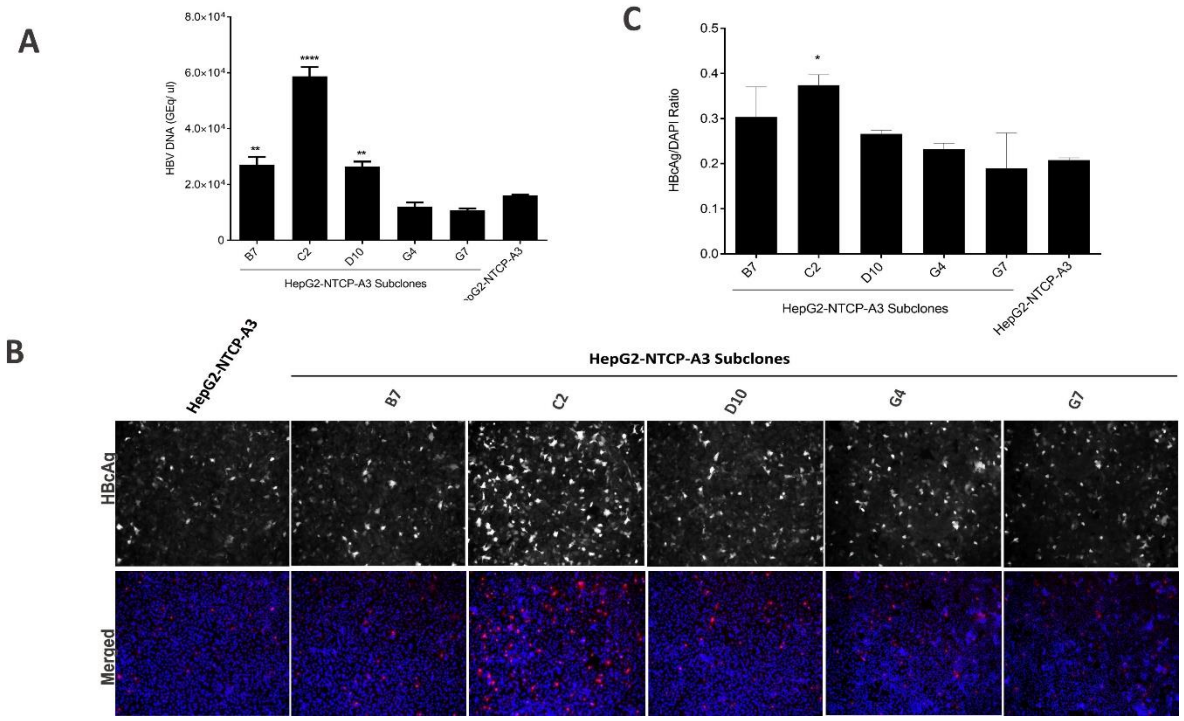

Figure 2: PEG-free HBV infection in HepG2-NTCP-A3 subclones. A). Indicated subclones of HepG2-NTCP-A3 were infected with HBV in PEG-free conditions and the amount of HBV DNA in the cell culture supernatant was quantified by real-time qPCR. B). PEG-free HBV infected cells were fixed and immunostained with HBcAg and counterstained with DAPI. The cells were visualized by fluorescence microscopy C). HBcAg fluorescence over DAPI shown as a ratio. Data are presented as mean±SD (One way ANOVA; $p < 0.0001$).

Preprints (www.preprints.org) | NOT PEER-REVIEWED | Posted: 14 July 2022 doi:10.20944/preprints202207.0220.v1

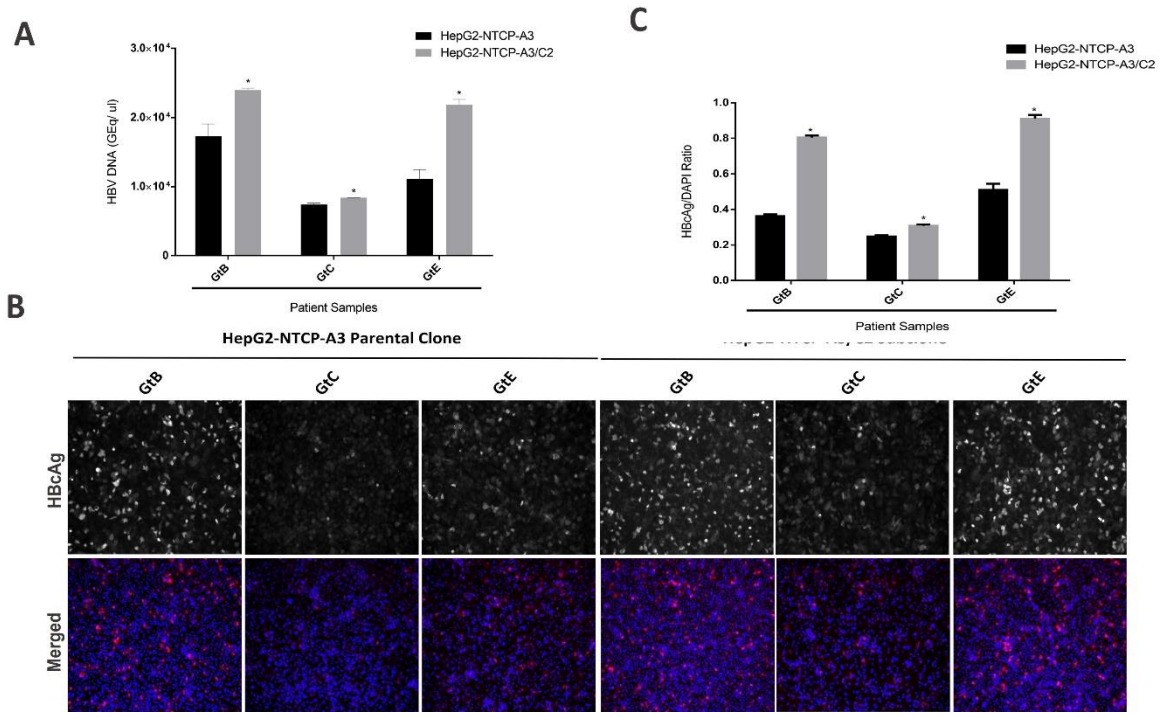

Figure 3: Susceptibility of C2 subclone to HBV Clinical isolates. HepG2-NTCP-A3 parental clone and C2 subclone were infected with three sequence confirmed genotype B, C and E patient samples. Supernatants were collected at day 7 post-infection and the amount of HBV DNA was quantified by real-time PCR. B). HBV infected cells were fixed and immunostained with an antibody to HBcAg and counterstained with DAPI. The cells were visualized by fluorescence microscopy C). HBcAg fluorescence over DAPI shown as a ratio. Data are presented as mean±SD (t-test; $p < 0.05$).

Preprints (www.preprints.org) | NOT PEER-REVIEWED | Posted: 14 July 2022 doi:10.20944/preprints202207.0220.v1

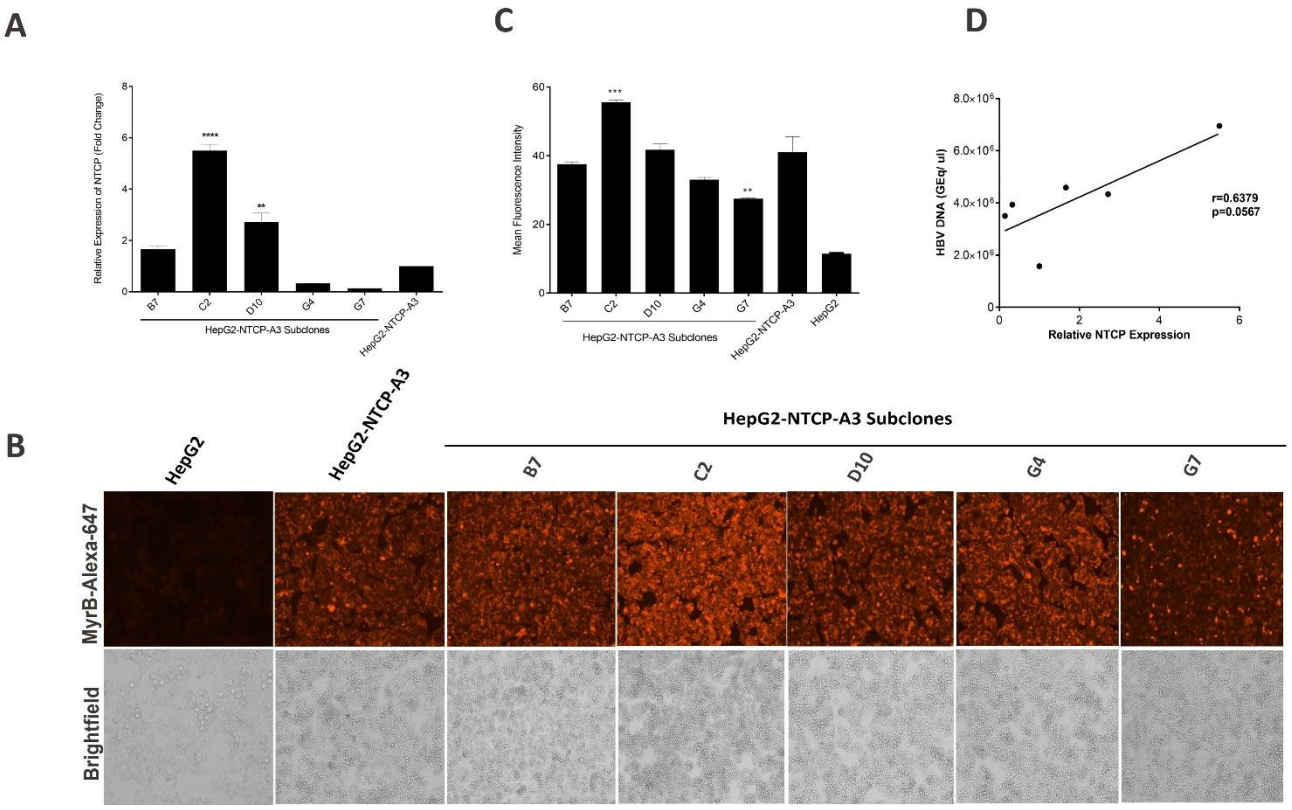

Figure 4: NTCP expression in subclones of HepG2-NTCP-A3 cells. A) HepG2-NTCP-A3 parental clone stably expressing human NTCP were subcloned by limiting dilution into 96-well plates. Individual subclones were expanded and processed for NTCP mRNA quantification by reverse transcriptase real time PCR. HepG2-NTCP-A3 parental clone was set to 1 and represented as a fold change and the data are presented as mean±SD (One way ANOVA; $p < 0.0001$) B). HepG2, HepG2-NTCP-A3 parental clone and its subclones B7, C2, D10, G4 and G7 were stained for cell surface NTCP expression using Alexa Fluor labelled Myrcludex B (MyrB-Alexa-647) and visualized by fluorescence microscopy C). Quantitative representation of cell surface NTCP expression as mean fluorescence intensity (MFI) D). Pearson correlation coefficient between NTCP expression levels and HBV infection in HepG2-NTCP-A3 parental clone and its subclones B7, C2, D10, G4 and G7.